Properties of Strained Structures and Topological Defects in Graphene

Jiong Lu,[†,‡] Yang Bao,[†,‡,§] Chen Liang Su,[†] and Kian Ping Loh[†,‡,*]

[†]Department of Chemistry, National University of Singapore, 3 Science Drive 3, Singapore 117543, and [‡]Graphene Research Centre, National University of Singapore, 6 Science Drive 2, Singapore 117546. [§]Present address: NUS Graduate School for Integrative Sciences and Engineering, 28 Medical Drive #05-01, Singapore 117597, Singapore and Graphene research center.

This Perspective is contributed by a recipient of the 2013 *ACS Nano* Lectureship Awards, presented at the International Conference on Nanoscience & Technology, China 2013 (ChinaNANO 2013) in September 2013. The *ACS Nano* Lectureship honors the contributions of scientists whose work has significantly impacted the fields of nanoscience and nanotechnology.

ABSTRACT Strain and defect engineering of graphene can modify the topological features of electronic states, leading to novel properties such as pseudomagnetism in bubbles and metallicity in extended topological defects. A consequence of graphene being a soft membrane is that it can be strain-engineered to become highly corrugated by modifying its adhesion to the substrate. Extended grain boundaries in graphene can be constructed from periodic combinations of nonhexagonal rings (5−7 pairs). However, a controlled method of producing these defects is not currently available. In this Perspective, we discuss some of the recent advances in studying the properties and formation mechanisms of strained structures and defects in graphene, extending across both physics and chemistry.

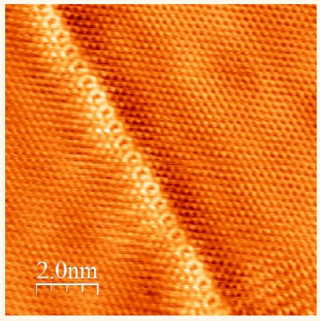

The remarkable electronic properties of graphene, such as its high carrier mobilities, linear dispersion of Dirac fermions, and high Fermi level tunability, make it potentially useful in high-speed microelectronics.[1−4] However, a large gap exists between the superlative properties predicted by theory and the actual performance of graphene. Ideal graphene is often represented as a flat membrane with virtually no defects. In reality, the material's elasticity renders its surface susceptible to deformation in the third dimension, which gives rise to strained structures such as ripples[5−7] and bubbles.[8−12] In addition to physical strains, the carbon atoms of graphene can be removed or rearranged during growth[13−15] or solution processing[16,17] such that voids or topological defects are introduced into the material. Although these defects degrade charge mobility, they are sometimes intentionally introduced to manipulate charge transport. Increasingly, experiment and theory indicate that the presence of defects or strained structures in graphene can alter its electronic or chemical properties in potentially useful ways.[14,18−20] However, for such alterations to be useful, researchers must first learn how to introduce these defects in controllable ways. To this end, we review recent studies on various defects and strained structures in graphene and discuss how these imperfections can impart novel electronic and chemical properties that are absent in the flat, pristine sheet.

Increasingly, experiment and theory indicate that the presence of defects or strained structures in graphene can alter its electronic or chemical properties in potentially useful ways.

Graphene has a tendency to crumple in the third dimension because of its large ratio of in-plane rigidity to bending rigidity.[5,8] In most cases, the substrate supporting graphene induces corrugations due either to the lattice mismatch or to the

* Address correspondence to chmlohkp@nus.edu.sg.

Published online October 22, 2013
10.1021/nn4051248

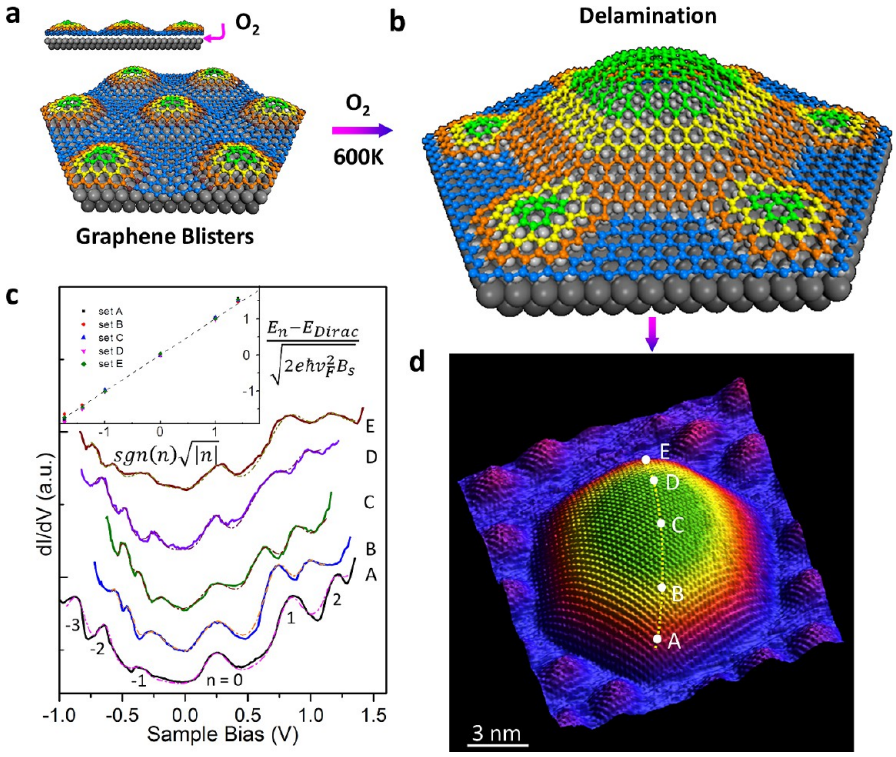

Figure 1. (a) Graphene blisters on graphene moiré superlattice on Ru(0001). (b) Formation of graphene nanobubbles (GNBs) by oxygen intercalation. (c) Sequence of five d*I*/d*V* spectra taken at A−E points: (d) black (A); blue (B), olive (C), violet (D), wine (E); dashed lines in c: Gaussian fit. Inset of (c): Normalized peak energy $(E_n - E_{Dirac})/(2e\hbar v_F^2 B_S)^{1/2}$ *versus* sgn(*n*)(|*n*|)$^{1/2}$ for Landau energy peaks (*n* = −3, ±2, ±1, 0) observed on A−E points of hexagonal GNB in d, which follow the expected scaling behavior from the equation (black, red, blue, magenta, olive sets corresponding to normalized peak energy in scanning tunneling spectroscopy curves of A−E, respectively). (d) Three-dimensional scanning tunneling microscopy of hexagonal graphene nanobubbles. Adapted with permission from ref 10. Copyright 2012 Nature Publishing Group.

different thermal expansion coefficients between graphene and the substrate.[21] Even in suspended graphene, which is free from the influence of a substrate, thermal fluctuations lead to spontaneous lattice deformation and the formation of intrinsic ripples.[5,6] The strain associated with such corrugations has been predicted to alter graphene band structures in two main ways: (i) lattice distortion shifts the on-site energy of p_z orbitals due to changes in the lattice constant between carbon ions; and (ii) lattice deformation modulates the electron-hopping amplitude between sublattices, giving rise to an effective gauge field that constricts the electron motion in graphene as if under the influence of a real magnetic field.[21−23] Strain engineering has been proposed as a method for manipulating graphene's electronic and optical properties and for enhancing interaction and correlation effects.[23] However, the bottleneck of strain engineering in graphene has been the ability to produce relatively large strain within a certain length scale. The typical graphene ripples observed on a SiO_2 substrate have height variations of 1−5 nm over a distance of 20−60 nm, giving rise to a random strain of 1%, which is too weak to induce the formation of a sufficiently large pseudomagnetic field.[21]

Coupling massless Dirac particles in graphene to strain *via* a pseudomagnetic field creates an electrodynamic environment that is solely dependent on the local deformations of the honeycomb lattice.[10] Random corrugation due to height variation of the underlying substrate is undesirable because it creates random fields and restricts the charge mobility in graphene due to flexural phonons.[7] Both theory and experimental observation have shown that only specific deformation patterns with trigonal symmetry are capable of producing uniform pseudomagnetic fields, as determined by the relationship between graphene's lattice symmetry and strain distributions.[22] Appropriately designed strain patterns with the correct symmetry are required for tuning the dynamics of carriers, which may enable novel applications of graphene. In this regard, we recently showed that geometrically precise strain texture in graphene can be engineered by controlling the adhesion of the graphene on a ruthenium (Ru) substrate. A buckling instability arising from the lattice mismatch between graphene and the substrate produces a graphene moiré superlattice. The graphene moiré superlattice consists of periodic undulations that form "valleys" and "humps" that resemble the surfaces of bubbles in bubble-wrap packaging (Figure 1a). As illustrated in Figure 1a, b, oxygen molecules were used as a

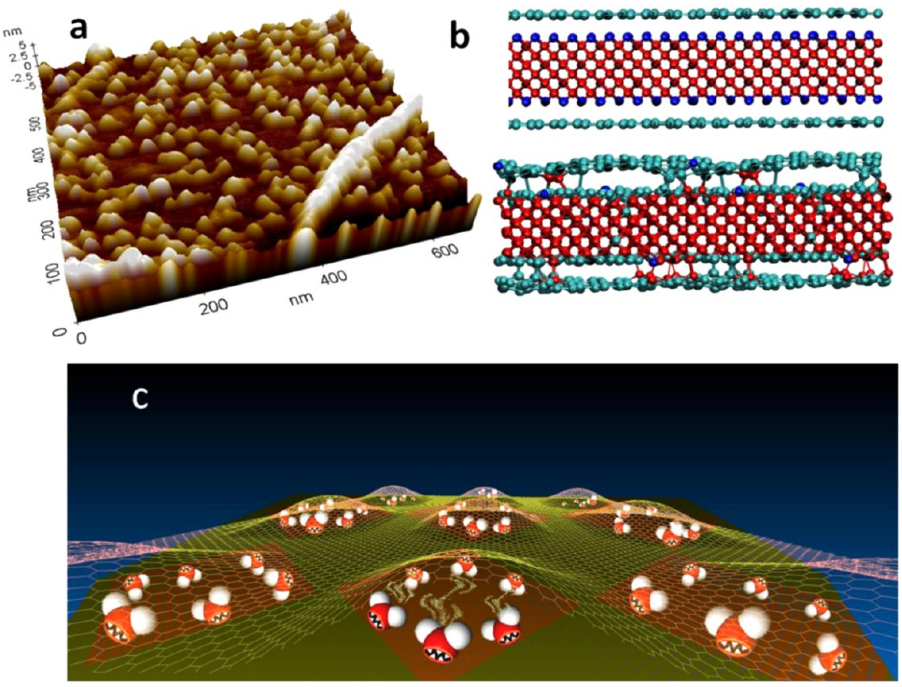

Figure 2. (a) Atomic force microscopy images of bubbles formed by thermally restructuring graphene on a diamond C(100) crystal. (b) Molecular dynamics simulation showing the covalent bonding that occurs between diamond and graphene after the dehydrogenation of the diamond surface at high temperature, which allows the edges of the bubbles to be sealed. (c) Sealed graphene bubbles on diamond act as a hydrothermal anvil cell, trapping supercritical fluid when heated to high temperatures.

reactive intercalant to delaminate the adhered graphene from the Ru substrate, such that graphene in the "hump" and "valley" regions sintered together to form a geometrically well-defined bubble whose edges follow the symmetry of the moiré superlattice. As the delamination process involves bond breakage and is thermally activated, the deterministic shape evolution of the bubble can be controlled by the reaction temperature. A pseudomagnetic field of hundreds of Tesla can be produced in graphene bubbles showing strains in the range of 10−15% (Figure 1c,d). Such an enormous pseudomagnetic field is not accessible by laboratory techniques. Scanning tunneling spectroscopy (STS) reveals Landau level peaks induced by the pseudomagnetic field. These peaks are shifted to higher energy in the regions of the bubbles with the highest strain (*i.e.*, the edges). These nanobubbles allow the manipulation of electronic properties of graphene, as well as the exploration of frontier physics in the high-field regimes.[9,10]

Strain in graphene does not break time reversal symmetry but does deform the Brillouin zone. Edge states and Landau levels are thus expected to coexist in graphene nanodots strained along three main crystallographic directions, which can be used to create graphene pseudomagnetic quantum dots.[22,24] Engineering a strained superlattice in graphene on insulating substrates seems promising as it may offer a new method for generating a periodic potential, whereby a sizable band gap may be opened in graphene. This band gap can be created by placing graphene on top of a prepatterned substrate with periodic arrays of nanoclusters, nanostripes, and nanotrenches, on which the formation of periodically corrugated graphene can be induced. One interesting possibility is the use of light or electrical energy to actuate expansion or contraction of the patterned nanostructures (such as piezoelectric materials), thus allowing the strain in graphene to be tuned.

It is worth mentioning that the curvature-induced rehybridization between the p_z and σ orbitals of carbon atoms may reshape the chemistry of graphene, such as by creating reactive sites for hydrogenation or by offering adsorption potential wells for trapping molecules.[25,26] In a bubble, for example, the outer (convex) face has a higher density of electrons compared to the inner (concave) face, which explains our previous observation that an array of graphene nanobubbles can have higher electrochemical activity than flat graphene.[8] Charge transfer in the direction normal to the basal plane of flat graphene is known to be particularly sluggish, due to anisotropic charge transport in the two-dimensional plane.

We find that graphene bubbles, when covalently bonded to a substrate such as diamond (Figure 2), act as liquid cells by entrapping fluid between the bubbles and the substrate.[8] Due to the graphene's impermeability, water trapped inside the bubbles can be heated to supercritical conditions without evaporating. Thus, the bubbles can serve as excellent optical windows and

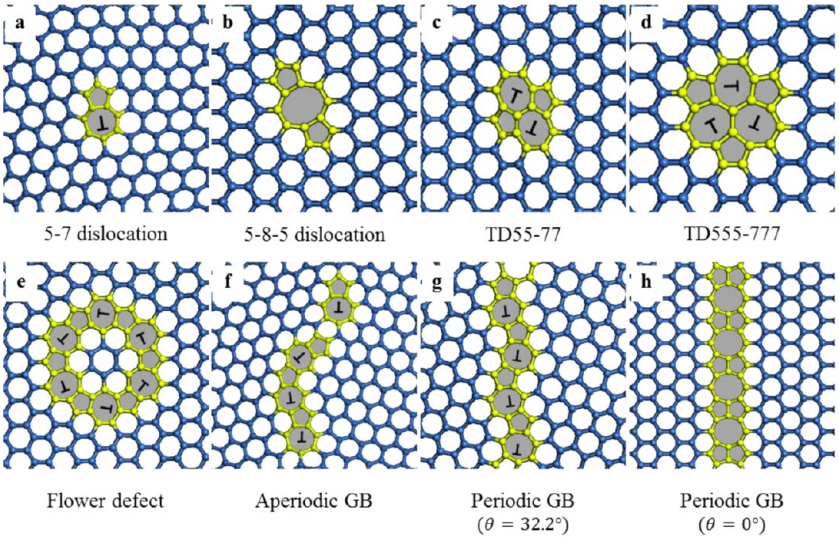

Figure 3. Structures of topological defects (TD) in graphene: (a) 5−7 dislocation; (b) 5−8−5 dislocation; (c) 55−77 clustered topological defect; (d) 555−777 clustered topological defect; (e) flower defect, which is a closed loop of 5−7 pairs. (f) Aperiodic grain boundary (GB); (g) $\theta = 32.2°$ periodic grain boundary; (h) $\theta = 0°$ periodic translational grain boundary.

liquid cells for studying high-pressure, high-temperature reactions.

Topological Defects and Periodic Grain Boundaries in Graphene. Structural defects in graphene are important because they strongly influence its physical and chemical properties, even at low concentrations. Unlike vacancies with dangling bonds or extrinsic dopants, intrinsic topological defects accommodate lattice imperfections (curvature or vacancies) but conserve the three-fold sp^2 bonding of carbon atoms. Plastic deformation of curved graphene sheets, as in fullerene or carbon nanotubes, as well as vacancies or grain boundaries, can induce topological defects. A topological defect is a local reconstruction of the hexagonal carbon lattice to form nonhexagonal carbon rings. These unique structures create new possibilities for extending the properties of graphene.

The simplest topological defects in graphene are disclinations (individual pentagons or heptagons).[27] They can be found in fullerenes and carbon nanotubes but appear less frequently in planar graphene because an individual disclination induces curvature in, and thus large strain on, the system. The pairing of a pentagon and a heptagon is energetically favorable due to curvature cancellation, which results in pentagon−heptagon (5−7) pairs (Figure 3a) known as dislocation cores.[28,29] Scanning tunneling microscopy (STM) and high-resolution transmission electron microscopy (HRTEM) have revealed 5−7 pair defects in both carbon nanotubes and graphene.[30−34] Besides individual 5−7 pairs, dislocation cores can also be found in clusters, which form complex structures, including the 55−77 defect (Stone-Wales defect, Figure 3c),[31,35−37] the 555−777 defect (Figure 3d),[33−35] and the flower defect (Figure 3e).[34,38] Other forms of nonhexagonal rings, such as the 5−8−5 defect (Figure 3b),[33,35] have also been identified experimentally. Individual or clustered topological defects can be found naturally in graphene grown using chemical vapor deposition,[30,32] epitaxial graphene on SiC,[36,38] or graphene generated *in situ* with HRTEM using the electron beam.[33−35,37]

> **Structural defects in graphene are important because they strongly influence its physical and chemical properties, even at low concentrations.**

Topological defects can modify the electronic properties of graphene by acting as scattering centers or as sources for self-doping.[14] Certain clustered topological defects (including topological defect 5555−6−7777) have been estimated to open a local band gap on the order of 200 meV.[35]

One interesting scenario is the alignment of individual or clustered topological defects into extended structures by taking advantage of the fact that there is a thermodynamic force for these defects to cluster together (Figure 4a). Recent experimental studies have identified topological defects (mostly 5−7 pairs) as building blocks for grain boundaries in polycrystalline graphene.[30,39] Grain boundaries constructed of extended topological defects not only give rise to entirely new properties but may also be integrated into practical devices. Chen and co-workers reported the synthesis of spatially ordered arrays of micrometer size grain boundaries and demonstrated device fabrication across a single grain boundary.[40]

Atomistic structures of grain boundaries have been discussed in a few theoretical papers.[29,41,42] In general, nonhexagonal rings such

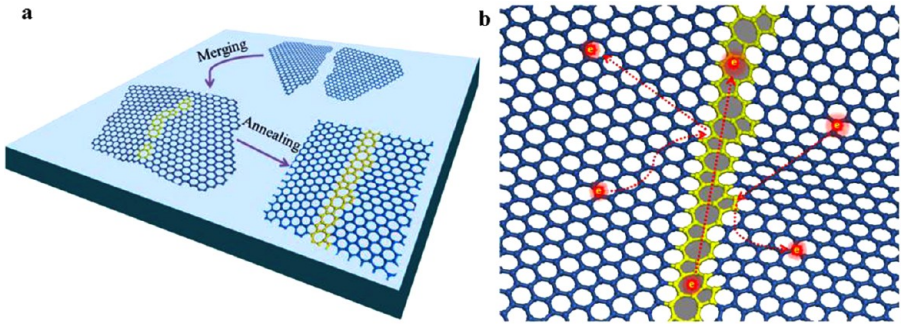

Figure 4. (a) Structural model showing how an aperiodic grain boundary is generated when two graphene islands merge, which transforms into a periodic grain boundary after annealing. (b) Charge transport in a periodic grain boundary—electrons moving across the grain boundary are reflected, whereas electrons moving along the boundary are transmitted.

as five-, seven-, and eight-membered rings can exist at grain boundaries to accommodate lattice mismatch between two graphene domains. For reasons similar to curvature cancellation, these rings pair to form dislocation cores. Although grain boundaries are often aperiodic (see Figure 3f), the ground-state grain boundary structures should contain periodic arrays of dislocation cores separated by hexagonal rings. The packing density of dislocation cores varies with the domain misorientation angle θ (ranging from 0 to 60° for graphene). For small-angle grain boundaries (θ close to zigzag direction at 0° or armchair direction at 60°), there is low packing density of topological defects, which leads to large separation between 5−7 pairs. The stress field of a 5−7 pair will induce out-of-plane buckling in graphene. This result is supported by STM images of graphene grown on Ir(111), where hillocks with large separations were observed at $\theta \approx 2°$ grain boundaries.[30] For large-angle grain boundaries (θ close to 30°) with high packing density of topological defects, stress fields associated with 5−7 pairs will mutually cancel each other, leading to structures with low formation energy. The theoretically calculated highest packing density occurs at $\theta = 32.2°$, with only 5−7 pairs (no hexagons) at the grain boundary region (see Figure 3g).[29,41] Although this structure contains the most defects, it has the lowest formation energy and the highest mechanical strength among all grain boundary structures, due to effective stress field cancellation.[29,41,43,44]

To date, most of the experimentally observed grain boundaries in graphene have been meandering and aperiodic.[39,45] These boundaries become electron scattering centers, which degrade the conductivity of the graphene sheet. Using STS, Biro and co-workers found that conductance at grain boundaries decreased by around 10-fold compared to the host graphene.[46] The self-doping effect has also been studied by STS, whereby grain boundaries had been found to exhibit higher electron affinity and exhibited stronger n-doping character than the host material, creating p-n-p or p-p′-p junctions across the grain boundary.[46,47] Louie and Yazyev proposed that low-energy charge carriers in graphene are either transmitted or reflected when crossing a grain boundary. For transmission across a periodic grain boundary, translational symmetry of the grain boundary requires momentum $k_{\|}$ parallel to the grain boundary to be conserved. Depending on the relative orientation of the graphene domains, conductance channels with given E and $K_{\|}$ on both sides of the grain boundary either match well or have significant misalignment (no momentum conservation) with each other. In the latter case, low-energy charge carriers are totally reflected by the grain boundary, which is equivalent to the presence of a transport gap. The transport gap depends solely on the dislocation core periodicity at the grain boundary. Simulation of a model reflective grain boundary (see Figure 4b) showed the on/off current ratio to be higher than 1000.[19] Hence, practical transistors could be built from tailored periodic grain boundaries. Periodic grain boundaries can also introduce van Hove singularities in the local density of states (DOS) of graphene within 0.5 eV of the Dirac point.[29] Electronic instability at van Hove singularities is believed to give rise to new phases with properties such as superconductivity, magnetism, and charge density waves.[48]

Lahiri and Batzill reported the first experimental observation of an extended grain boundary composed of paired pentagon and octagon rings (5−8−5) (Figure 3h) in a layer of graphene on nickel.[49] Simulation showed that this line defect was metallic in the longitudinal direction, which allowed it to act as a metallic wire for nanodevice applications. A small magnetic moment was calculated for each unit cell of the 5−8−5 grain boundary and was shown to increase under strain.[50] This increase suggests that the 5−8−5 grain boundary may be ferromagnetic. It is also predicted that this structure will exhibit two degenerate valleys at the Fermi level, which can be used as a valley filter in graphene valleytronics.[51]

Chemical Reactivity of Defects in Graphene. While the physical, electronic, and magnetic properties of the defects in graphene have been the subject of intense research interest from physicists,[18,52] the potential applications

of porous aromatic scaffolds in chemistry have not escaped the attention of chemists. Solution-processed graphene oxide (GO), which is made by treating graphite with strong oxidants and acids, can be considered to be the insulating, disordered analogue of the highly conducting crystalline graphene.[16,17,53] In contrast to early efforts on healing defects on GO in order to transform it into highly conductive graphene, increasing attention is now devoted to the introduction and enlargement of defects to enhance useful properties like catalysis,[53,54] sensing,[55,56] energy storage, and energy transfer.[57−59] In terms of chemical reactivity, the presence of defects in the form of holes, vacancies, or dislocations created in the basal plane during its preparation endow GO with redox-active carboxylic and quinone diols. These functional groups allow it to function as a solid acid and/or metal-free catalyst[60,61] for oxidative dehydrogenation (ODH) reactions. These defects can be intentionally created and enlarged by specific chemical treatment.[54,59,62] Unpaired spins are likely to be created in these defects and can enhance chemical reactivity and magnetic properties.[54]

In contrast to early efforts on healing defects on GO in order to transform it into highly conductive graphene, increasing attention is now devoted to the introduction and enlargement of defects to enhance useful properties like catalysis, sensing, energy storage, and energy transfer.

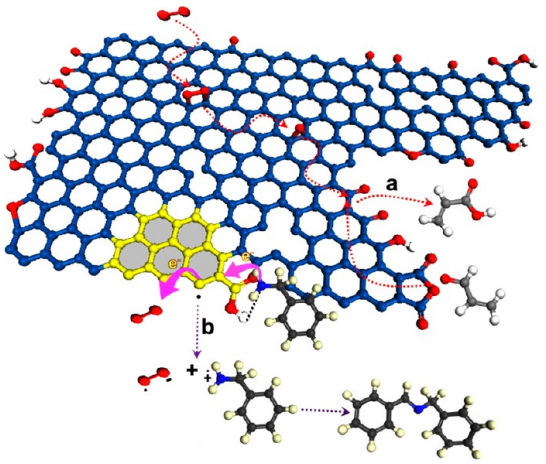

Figure 5. Voids and edge defects are decorated by catalytically active functional groups like carboxylic, quinones, diols, and unpaired spins. Small molecules such as oxygen (red dumbbell) are activated at these sites for subsequent oxidative reactions. Organic molecules that bind to these reactive defect sites become catalytically transformed. The diagram illustrates the oxidative coupling of amines.[54]

Defective graphitic structures have shown remarkable catalytic properties in gas-phase oxidation (Figure 5, pathway a).[60,61] Bao and co-workers[63] suggested that for liquid-phase reactions, the zigzag edges of rGO could act as the catalytically active sites for hydrogenation of nitrobenzene. They observed that the catalytic yield increased with the density of defects created by treatment with nitric acid. We recently discovered a sequential base and acid treatment that can create and enlarge the defects in GO and impart on it enhanced catalytic activities in the liquid-phase oxidative coupling of amines to imines (up to 98% yield and 5 wt % catalyst loading under solvent-free, open-air conditions).[54] The catalytic activity and stability of holey GO exceeds several types of noble metal catalysts.[64,65] We further examined the origin of this catalytic behavior, which was linked to the synergistic effect of carboxylic acid groups and unpaired spins at edge defects (Figure 5, pathway b).[54] The discovery of a simple chemical processing step to synthesize highly catalytically active GO opens the possibility of industrial scale carbocatalysis.

The enhanced interactions of gas molecules and defects in graphene materials can also be used in the chemical sensing of toxic gases. For example, Huang *et al.*[55] reported that hydrothermal steaming of GO created an electrically conductive, nanoporous rGO network *via* an oxidative etching process. The degree of etching and resultant porosity can be controlled by varying the reaction time. Compared to nonporous reduced GO, the nanoporous rGO shows an almost 2 orders of magnitude increase in sensitivity and improved recovery time for NO_2 detection.

OUTLOOK AND CHALLENGES

Pristine graphene may not be the ideal material for some applications because its charge transport is highly anisotropic, which renders sluggish charge transport out of plane. The gapless nature of pristine graphene is also a major drawback in electronics. Engineering defects into graphene, in the form of strained structures or voids, is one way of opening up new possibilities for its use in electronics and chemistry. To this end, it is vital to investigate how strained structures or topological defects, which typically emerge at random, can be created and assembled on graphene in a controlled manner. Nonhexagonal rings in graphene may be used

as building blocks for a new type of carbon architecture that incorporates designed curvature. Grain boundaries and defects may serve as atomic-scale filters for atoms and molecules or act as sites of controlled chemical reactions. Device scientists should consider exploiting strain or topological defects in graphene to create electronic junctions. Thus, defect engineering in graphene, as in bulk solid-state materials, may emerge as an important research field.

Conflict of Interest: The authors declare no competing financial interest.

Acknowledgment. K.P.L. acknowledges the Singapore Millennium Foundation Research Horizon Award (SMA-RHA R-143-001-417-133).

REFERENCES AND NOTES

1. Novoselov, K. S.; Geim, A. K.; Morozov, S. V.; Jiang, D.; Zhang, Y.; Dubonos, S. V.; Grigorieva, I. V.; Firsov, A. A. Electric Field Effect in Atomically Thin Carbon Films. *Science* **2004**, *306*, 666–669.
2. Castro Neto, A. H.; Guinea, F.; Peres, N. M. R.; Novoselov, K. S.; Geim, A. K. The Electronic Properties of Graphene. *Rev. Mod. Phys.* **2009**, *81*, 109–162.
3. Novoselov, K. S.; Geim, A. K.; Morozov, S. V.; Jiang, D.; Katsnelson, M. I.; Grigorieva, I. V.; Dubonos, S. V.; Firsov, A. A. Two-Dimensional Gas of Massless Dirac Fermions in Graphene. *Nature* **2005**, *438*, 197–200.
4. Liao, L.; Lin, Y. C.; Bao, M. Q.; Cheng, R.; Bai, J. W.; Liu, Y. A.; Qu, Y. Q.; Wang, K. L.; Huang, Y.; Duan, X. F. High-Speed Graphene Transistors with a Self-Aligned Nanowire Gate. *Nature* **2010**, *467*, 305–308.
5. Fasolino, A.; Los, J. H.; Katsnelson, M. I. Intrinsic Ripples in Graphene. *Nat. Mater.* **2007**, *6*, 858–861.
6. Bao, W. Z.; Miao, F.; Chen, Z.; Zhang, H.; Jang, W. Y.; Dames, C.; Lau, C. N. Controlled Ripple Texturing of Suspended Graphene and Ultrathin Graphite Membranes. *Nat. Nanotechnol.* **2009**, *4*, 562–566.
7. Ni, G.-X.; Zheng, Y.; Bae, S.; Kim, H. R.; Pachoud, A.; Kim, Y. S.; Tan, C.-L.; Im, D.; Ahn, J.-H.; Hong, B. H.; *et al.* Quasi-Periodic Nanoripples in Graphene Grown by Chemical Vapor Deposition and Its Impact on Charge Transport. *ACS Nano* **2012**, *6*, 1158–1164.
8. Lim, C. H. Y. X.; Sorkin, A.; Bao, Q.; Li, A.; Zhang, K.; Nesladek, M.; Loh, K. P. A Hydrothermal Anvil Made of Graphene Nanobubbles on Diamond. *Nat. Commun.* **2013**, *4*, 1556.
9. Levy, N.; Burke, S. A.; Meaker, K. L.; Panlasigui, M.; Zettl, A.; Guinea, F.; Castro Neto, A. H.; Crommie, M. F. Strain-Induced Pseudo-Magnetic Fields Greater than 300 T in Graphene Nanobubbles. *Science* **2010**, *329*, 544–547.
10. Lu, J.; Castro Neto, A. H.; Loh, K. P. Transforming Moiré Blisters into Geometric Graphene Nano-Bubbles. *Nat. Commun.* **2012**, *3*, 823.
11. Georgiou, T.; Britnell, L.; Blake, P.; Gorbachev, R. V.; Gholinia, A.; Geim, A. K.; Casiraghi, C.; Novoselov, K. S. Graphene Bubbles with Controllable Curvature. *Appl. Phys. Lett.* **2011**, *99*, 093103.
12. Stolyarova, E.; Stolyarov, D.; Bolotin, K.; Ryu, S.; Liu, L.; Rim, K. T.; Klima, M.; Hybertsen, M.; Pogorelsky, I.; Pavlishin, I.; *et al.* Observation of Graphene Bubbles and Effective Mass Transport under Graphene Films. *Nano Lett.* **2009**, *9*, 332–337.
13. Ugeda, M. M.; Fernandez-Torre, D.; Brihuega, I.; Pou, P.; Martinez-Galera, A. J.; Perez, R.; Gomez-Rodriguez, J. M. Point Defects on Graphene on Metals. *Phys. Rev. Lett.* **2011**, *107*, 116803.
14. Banhart, F.; Kotakoski, J.; Krasheninnikov, A. V. Structural Defects in Graphene. *ACS Nano* **2011**, *5*, 26–41.
15. Lu, J.; Yeo, P. S. E.; Gan, C. K.; Wu, P.; Loh, K. P. Transforming C_{60} Molecules into Graphene Quantum Dots. *Nat. Nanotechnol.* **2011**, *6*, 247–252.
16. Loh, K. P.; Bao, Q.; Ang, P. K.; Yang, J. The Chemistry of Graphene. *J. Mater. Chem.* **2010**, *20*, 2277–2289.
17. Loh, K. P.; Bao, Q.; Eda, G.; Chhowalla, M. Graphene Oxide as a Chemically Tunable Platform for Optical Applications. *Nat. Chem.* **2010**, *2*, 1015–1024.
18. Carr, L. D.; Lusk, M. T. Defect Engineering: Graphene Gets Designer Defects. *Nat. Nanotechnol.* **2010**, *5*, 316–317.
19. Yazyev, O. V.; Louie, S. G. Electronic Transport in Polycrystalline Graphene. *Nat. Mater.* **2010**, *9*, 806–809.
20. Elias, D. C.; Nair, R. R.; Mohiuddin, T. M. G.; Morozov, S. V.; Blake, P.; Halsall, M. P.; Ferrari, A. C.; Boukhvalov, D. W.; Katsnelson, M. I.; Geim, A. K.; *et al.* Control of Graphene's Properties by Reversible Hydrogenation: Evidence for Graphane. *Science* **2009**, *323*, 610–613.
21. Guinea, F. Strain Engineering in Graphene. *Solid State Commun.* **2012**, *152*, 1437–1441.
22. Guinea, F.; Katsnelson, M. I.; Geim, A. K. Energy Gaps and a Zero-Field Quantum Hall Effect in Graphene by Strain Engineering. *Nat. Phys.* **2010**, *6*, 30–33.
23. Pereira, V. M.; Neto, A. H. C. Strain Engineering of Graphene's Electronic Structure. *Phys. Rev. Lett.* **2009**, *103*, 046801.
24. Qi, Z.; Bahamon, D. A.; Pereira, V. M.; Park, H. S.; Campbell, D. K.; Neto, A. H. C. Resonant Tunneling in Graphene Pseudomagnetic Quantum Dots. *Nano Lett.* **2013**, *13*, 2692–2697.
25. Wang, Z. F.; Zhang, Y.; Liu, F. Formation of Hydrogenated Graphene Nanoripples by Strain Engineering and Directed Surface Self-Assembly. *Phys. Rev. B* **2011**, *83*, 041403(R).
26. Lu, J.; Yeo, P. S. E.; Zheng, Y.; Yang, Z.; Bao, Q.; Gan, C. K.; Loh, K. P. Using the Graphene Moiré Pattern for the Trapping of C-60 and Homoepitaxy of Graphene. *ACS Nano* **2012**, *6*, 944–950.
27. Saito, R.; Dresselhaus, G.; Dresselhaus, M. S. Topological Defects in Large Fullerenes. *Chem. Phys. Lett.* **1992**, *195*, 537–542.
28. Liu, Y.; Yakobson, B. I. Cones, Pringles, and Grain Boundary Landscapes in Graphene Topology. *Nano Lett.* **2010**, *10*, 2178–2183.
29. Yazyev, O. V.; Louie, S. G. Topological Defects in Graphene: Dislocations and Grain Boundaries. *Phys. Rev. B* **2010**, *81*, 195420.
30. Coraux, J.; N'Diaye, A. T.; Busse, C.; Michely, T. Structural Coherency of Graphene on Ir(111). *Nano Lett.* **2008**, *8*, 565–570.
31. Suenaga, K.; Wakabayashi, H.; Koshino, M.; Sato, Y.; Urita, K.; Iijima, S. Imaging Active Topological Defects in Carbon Nanotubes. *Nat. Nanotechnol.* **2007**, *2*, 358–360.
32. Warner, J. H.; Margine, E. R.; Mukai, M.; Robertson, A. W.; Giustino, F.; Kirkland, A. I. Dislocation-Driven Deformations in Graphene. *Science* **2012**, *337*, 209–212.
33. Lehtinen, O.; Kurasch, S.; Krasheninnikov, A. V.; Kaiser, U. Atomic Scale Study of the Life Cycle of a Dislocation in Graphene from Birth to Annihilation. *Nat. Commun.* **2013**, *4*, 2098.
34. Kurasch, S.; Kotakoski, J.; Lehtinen, O.; Skákalová, V.; Smet, J.; Krill, C. E.; Krasheninnikov, A. V.; Kaiser, U. Atom-by-Atom Observation of Grain Boundary Migration in Graphene. *Nano Lett.* **2012**, *12*, 3168–3173.
35. Kotakoski, J.; Krasheninnikov, A. V.; Kaiser, U.; Meyer, J. C. From Point Defects in Graphene to Two-Dimensional Amorphous Carbon. *Phys. Rev. Lett.* **2011**, *106*, 105505.
36. Meyer, J. C.; Kisielowski, C.; Erni, R.; Rossell, M. D.; Crommie, M. F.; Zettl, A. Direct Imaging of Lattice Atoms and Topological Defects in Graphene Membranes. *Nano Lett.* **2008**, *8*, 3582–3586.
37. Girit, Ç. Ö.; Meyer, J. C.; Erni, R.; Rossell, M. D.; Kisielowski, C.; Yang, L.; Park, C.-H.; Crommie, M. F.; Cohen, M. L.; Louie, S. G.; *et al.* Graphene at the Edge: Stability and Dynamics. *Science* **2009**, *323*, 1705–1708.
38. Cockayne, E.; Rutter, G. M.; Guisinger, N. P.; Crain, J. N.; First, P. N.; Stroscio, J. A. Grain Boundary Loops in Graphene. *Phys. Rev. B* **2011**, *83*, 195425.
39. Huang, P. Y.; Ruiz-Vargas, C. S.; van der Zande, A. M.; Whitney, W. S.; Levendorf, M. P.; Kevek, J. W.; Garg,

S.; Alden, J. S.; Hustedt, C. J.; Zhu, Y.; *et al.* Grains and Grain Boundaries in Single-Layer Graphene Atomic Patchwork Quilts. *Nature* **2011**, *469*, 389–392.
40. Yu, Q.; Jauregui, L. A.; Wu, W.; Colby, R.; Tian, J.; Su, Z.; Cao, H.; Liu, Z.; Pandey, D.; Wei, D.; *et al.* Control and Characterization of Individual Grains and Grain Boundaries in Graphene Grown by Chemical Vapour Deposition. *Nat. Mater.* **2011**, *10*, 443–449.
41. Carlsson, J. M.; Ghiringhelli, L. M.; Fasolino, A. Theory and Hierarchical Calculations of the Structure and Energetics of [0001] Tilt Grain Boundaries in Graphene. *Phys. Rev. B* **2011**, *84*, 165423.
42. Liu, T.-H.; Gajewski, G.; Pao, C.-W.; Chang, C.-C. Structure, Energy, and Structural Transformations of Graphene Grain Boundaries from Atomistic Simulations. *Carbon* **2011**, *49*, 2306–2317.
43. Grantab, R.; Shenoy, V. B.; Ruoff, R. S. Anomalous Strength Characteristics of Tilt Grain Boundaries in Graphene. *Science* **2010**, *330*, 946–948.
44. Wei, Y.; Wu, J.; Yin, H.; Shi, X.; Yang, R.; Dresselhaus, M. The Nature of Strength Enhancement and Weakening by Pentagon−Heptagon Defects in Graphene. *Nat. Mater.* **2012**, *11*, 759–763.
45. Kim, K.; Lee, Z.; Regan, W.; Kisielowski, C.; Crommie, M. F.; Zettl, A. Grain Boundary Mapping in Polycrystalline Graphene. *ACS Nano* **2011**, *5*, 2142–2146.
46. Tapaszto, L.; Nemes-Incze, P.; Dobrik, G.; Yoo, K. J.; Hwang, C.; Biro, L. P. Mapping the Electronic Properties of Individual Graphene Grain Boundaries. *Appl. Phys. Lett.* **2012**, *100*, 053114-4.
47. Koepke, J. C.; Wood, J. D.; Estrada, D.; Ong, Z.-Y.; He, K. T.; Pop, E.; Lyding, J. W. Atomic-Scale Evidence for Potential Barriers and Strong Carrier Scattering at Graphene Grain Boundaries: A Scanning Tunneling Microscopy Study. *ACS Nano* **2012**, *7*, 75–86.
48. Li, G.; Luican, A.; Lopes dos Santos, J. M. B.; Castro Neto, A. H.; Reina, A.; Kong, J.; Andrei, E. Y. Observation of van Hove Singularities in Twisted Graphene Layers. *Nat. Phys.* **2010**, *6*, 109–113.
49. Lahiri, J.; Lin, Y.; Bozkurt, P.; Oleynik, I. I.; Batzill, M. An Extended Defect in Graphene as a Metallic Wire. *Nat. Nanotechnol.* **2010**, *5*, 326–329.
50. Kou, L.; Tang, C.; Guo, W.; Chen, C. Tunable Magnetism in Strained Graphene with Topological Line Defect. *ACS Nano* **2011**, *5*, 1012–1017.
51. Gunlycke, D.; White, C. T. Graphene Valley Filter Using a Line Defect. *Phys. Rev. Lett.* **2011**, *106*, 136806.
52. Terrones, H.; Lv, R. T.; Terrones, M.; Dresselhaus, M. S. The Role of Defects and Doping in 2D Graphene Sheets and 1D Nanoribbons. *Rep. Prog. Phys.* **2012**, *75*, 062501.
53. Su, C.; Loh, K. P. Carbocatalysts: Graphene Oxide and Its Derivatives. *Acc. Chem. Res.* **2013**, *46*, 2275–2285.
54. Su, C.; Acik, M.; Takai, K.; Lu, J.; Hao, S.; Zheng, Y.; Wu, P.; Bao, Q.; Enoki, T.; Chabal, Y. J.; *et al.* Probing the Catalytic Activity of Porous Graphene Oxide and the Origin of This Behaviour. *Nat. Commun.* **2012**, *3*, 1298.
55. Han, T.; Huang, Y.; Tan, A. T. L.; Dravid, V. P.; Huang, J. Steam Etched Porous Graphene Oxide Network for Chemical Sensing. *J. Am. Chem. Soc.* **2011**, *133*, 15264–15267.
56. Yuan, W.; Shi, G. Graphene-Based Gas Sensors. *J. Mater. Chem. A* **2013**, *1*, 10078–10091.
57. Zhu, Y.; Murali, S.; Stoller, M. D.; Ganesh, K. J.; Cai, W.; Ferreira, P. J.; Pirkle, A.; Wallace, R. M.; Cychosz, K. A.; Thommes, M.; *et al.* Carbon-Based Supercapacitors Produced by Activation of Graphene. *Science* **2011**, *332*, 1537–1541.
58. Zhang, L.; Zhao, X.; Stoller, M. D.; Zhu, Y.; Ji, H.; Murali, S.; Wu, Y.; Perales, S.; Clevenger, B.; Ruoff, R. S. Highly Conductive and Porous Activated Reduced Graphene Oxide Films for High-Power Supercapacitors. *Nano Lett.* **2012**, *12*, 1806–1812.
59. Zhao, X.; Hayner, C. M.; Kung, M.; Kung, H. Flexible Holey Graphene Paper Electrodes with Enhanced Rate Capability for Energy Storage Applications. *ACS Nano* **2011**, *5*, 8739–8749.
60. Su, D.; Perathoner, S.; Centi, G. Nanocarbons for the Development of Advanced Catalysts. *Chem. Rev.* **2013**, *113*, 5782–5816.
61. Su, D.; Zhang, J.; Frank, B.; Thomas, A.; Wang, X.; Paraknowitsch, J.; Schlogl, R. Metal-Free Heterogeneous Catalysis for Sustainable Chemistry. *ChemSusChem* **2010**, *3*, 169–180.
62. Wang, X.; Jiao, L. Y.; Sheng, K.; Li, C.; Dai, L.; Shi, G. Solution-Processable Graphene Nanomeshes with Controlled Pore Structures. *Sci. Rep.* **2013**, *3*, 1996.
63. Gao, Y.; Ma, D.; Wang, C.; Guan, J.; Bao, X. Reduced Graphene Oxide as a Catalyst for Hydrogenation of Nitrobenzene at Room Temperature. *Chem. Commun.* **2011**, *47*, 2432–2434.
64. Prades, A.; Peris, E.; Albrecht, M. Oxidations and Oxidative Couplings Catalyzed by Triazolylidene Ruthenium Complexes. *Organometallics* **2011**, *30*, 1162–1167.
65. Grirrane, A.; Corma, A.; Garcia, H. Highly Active and Selective Gold Catalysts for the Aerobic Oxidative Condensation of Benzylamines to Imines and One-Pot, Two-Step Synthesis of Secondary Benzylamines. *J. Catal.* **2009**, *264*, 138–144.